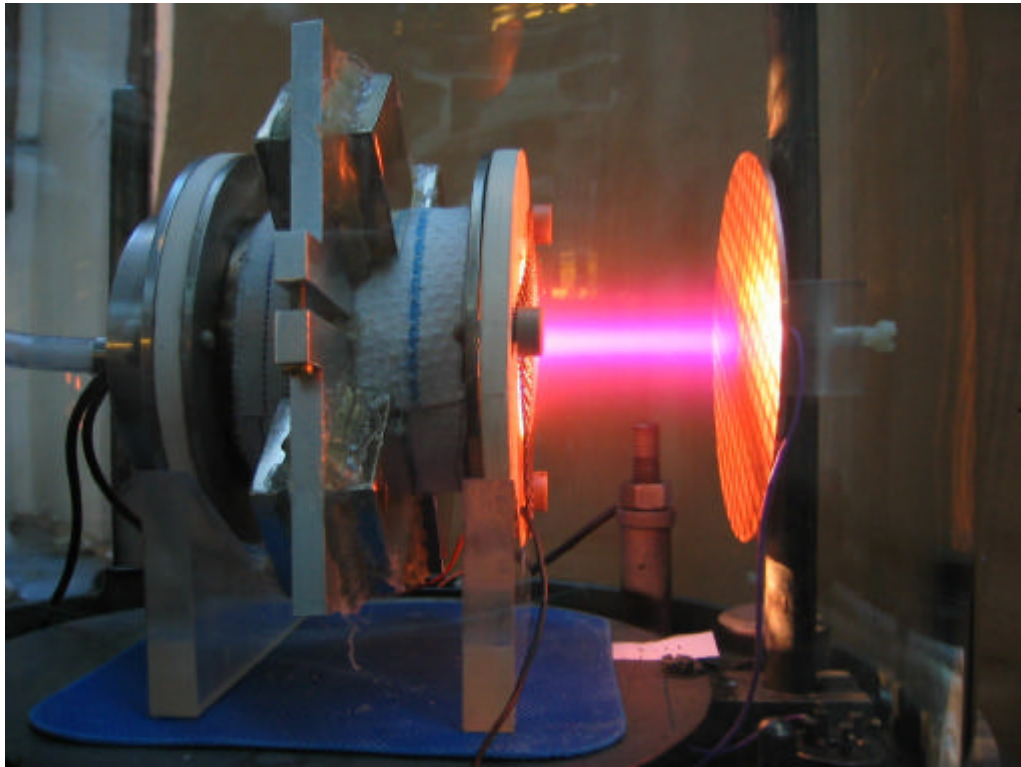


Investigation into the factors affecting the performance of an Electrostatic Ion Thruster

David Wilson
MPHYS 2003



Written by David Wilson (MPHYS) 2003
Supervisor: Professor Newport

Acknowledgements

I'd like to express a huge amount of thanks to Jay Day from the Part II lab for the incredible amount of help and support he has given me throughout the course of this project. Without his knowledge and experience this project wouldn't have been possible.

The brilliant manufacturing of the thruster was thanks to Don Riley and Co. from the mechanical workshop – an invaluable research tool that will be greatly missed.

Final thanks to my Supervisor Professor Newport for daringly allowing me this project, Professor Brown, Dr. Evans, Nathan Routley from the NMR department and Peter Verral from Technical services.

Contents

2	Introduction	4
3	Theory	7
4	Design and Construction	12
	4.1 Design Schematic	12
	4.2 Thruster design	13
	4.3 Cathode arrangement	14
5	Magnetic containment	16
	5.1 Magnet orientation	16
	5.2 Femme Modelling	17
	5.3 Hall probe verification	18
	5.4 Fortran Modelling	19
6	Optimal thruster configuration	21
7	Temperature testing	23
8	Experimental procedure	24
9	Results	26
	9.1 No magnetic field	26
	9.2 Full magnetic field (4 magnets)	30
	9.3 Fine mesh accelerating grid	32
	9.4 Effect of collector distance	33
	9.5 Reduced magnetic field (2 magnets)	33
	9.6 Multiple accelerating grid arrangements	33
10	Sources of error	35
11	Conclusions	37
	References	38

1 Abstract

As more daring explorative missions to the outer solar system are conceived the need arises for more efficient propulsion systems. Electrostatic propulsion is considered the most promising and in this project I have investigated the technology and through a design, construction and testing method I have determined the factors that affect the performance of such a thruster.

From existing literature I have designed and constructed a micro-ion thruster, modular in design to allow the testing of a wide range of configurations and parameters.

The thruster was tested in the Edwards evaporating unit in the part II lab using nitrogen (for convenience) as a propellant. A Faraday type collector was used to measure the output ion beam current which is proportional to thrust. A variety of factors were investigated including propellant flow rate, discharge current and voltage and the effect of an external magnetic field to extend the electron path length increasing the ionisation probability.

It was found that the performance of the thruster was controlled by a complex interaction of a variety of interdependent variables. The most notable of these was electron containment through the application a strong axial magnetic field.

A modest thrust was achieved by the thruster but it was significantly lower than the theoretical maximum of the design and at a low efficiency. Many sources of loss were identified that could, with further investigation, be reduced.

Overall it was found that to produce a high performance thruster capable of working at high efficiencies it is necessary to have a greater understanding of the interaction of the magnetic and electric fields with the physical thruster design.

2 Introduction

Chemical rockets work by reacting chemicals to create a hot expanding gas, which when expelled creates thrust.¹ The amount of thrust produced is related to the amount of propellant consumed and the Specific Impulse (I_{sp}) of the propellant.^a Specific Impulse is an engineering term with units of seconds. It can be defined as the Impulse given to a spacecraft per unit weight of propellant used. The more ‘energetic’ the propellant, the higher it’s specific impulse. It is always, therefore, a rocket scientist’s aim to maximise specific impulse.

According to Newton’s laws of motion the thrust of a rocket is given by,

$$F = mv_e = mgI_{sp}$$

Where F = thrust, v_e = effective exhaust velocity, m = propellant mass burnt and g = acceleration due to gravity.

Total impulse is given by the integral of thrust over time:

$$I = \int Fdt$$

Where I = total Impulse.

Specific Impulse is directly proportional to exhaust velocity and so higher Specific Impulses lead to higher thrust and greater total Impulse.

These equations lead to Tsiolkovsky’s rocket equation:

$$\Delta V = v_e \log_e \frac{M_o}{M}, \text{ re-arranging, } \frac{M}{M_o} = e^{-\Delta V / v_e}$$

Where V = spacecraft velocity, M_o = initial spacecraft mass and M = final spacecraft mass. This rocket equation is the backbone of rocket theory as it shows that a change in spacecraft velocity, ΔV , is dependent on exhaust velocity and propellant mass consumed. The re-arrangement shows that for a spacecraft to deliver a sizeable portion of its initial mass to its destination the propellant exhaust velocity must be comparable to the velocity change, ΔV .

Although chemical energies are huge, the simple rocket system is limited in that it cannot produce more energy than is chemically contained within the propellants – no more energy can

^a Although I have called it the Specific Impulse of the propellant it is more accurately the Specific Impulse of the engine as engine design and performance affect its value.

be added. At present the most powerful chemical rockets are liquid O₂/H₂ which can produce exhaust velocities of up to 4.5 km/sec. Unfortunately these rockets are complex requiring bulky valves and control systems and heavy cryogenic tanks. These have to be lifted into earth orbit at huge expense.

As more daring interplanetary missions are devised and manned missions to Mars considered it has become apparent that higher performance propulsion systems are required that can produce propellant exhaust velocities far in excess of the 4.5 km/sec available from chemical rockets.

Solar sails are presently impractical and limited to inner solar system travel and environmental concerns have limited nuclear propulsion. Another possibility is Electric Propulsion. Proposed in 1906 by Robert Goddard² it has only recently come into common usage as space technology has developed.^a It is now used for spacecraft station keeping and increasingly for interplanetary spacecraft propulsion such as NASA's Deep Space 1 comet rendezvous mission. Electric propulsion is now under intensive development across the world where the aim is to produce larger and more efficient (higher I_{sp}) thrusters ready for ever more demanding space missions.

The basic idea is to expel a propellant from the spacecraft by applying electrical energy, creating a stream of particles with an exhaust velocity significantly higher than that produced by chemical means. Electric propulsion requires a far smaller quantity of propellant without the need for bulky cryogenic containment and provided the electrical conditioning systems are small enough allows for lighter, cheaper missions or a greater payload mass. Electrical energy can easily be obtained from solar cells or for deep space missions from a compact RTG (Radioisotopic Thermoelectric Generator). The thruster can be switched on or off as desired and by altering the power input can be 'throttled' for performing manoeuvres. Due to 'space charge' limits, however, electric propulsion can only provide a very small thrust but by leaving the thruster operating for extended periods large total impulses can be achieved. For this reason, however, it will never replace chemical rockets but can provide an efficient, cost effective alternative for long duration deep space missions requiring high velocity increments³.

^a Excluding undocumented use by Russia.

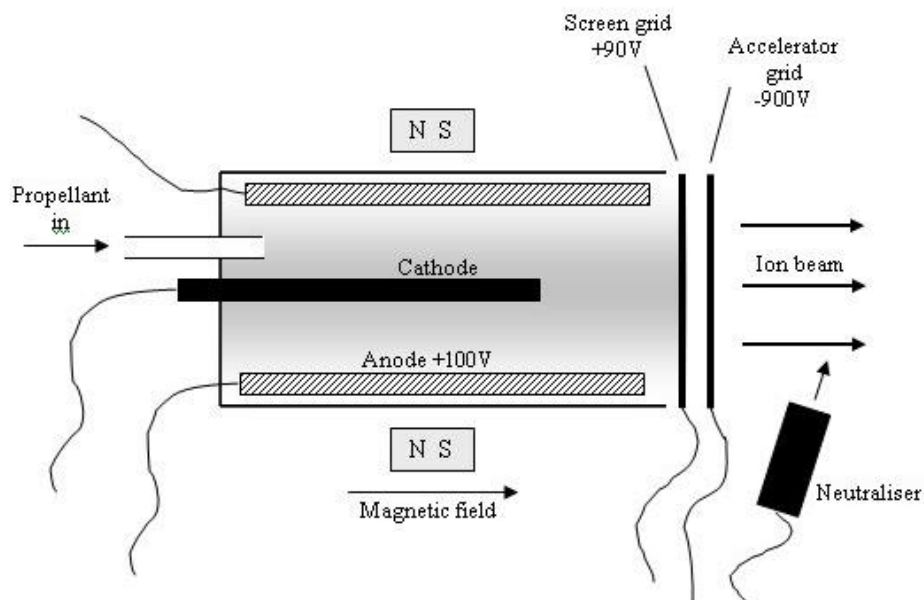
Several methods of particle acceleration are possible including electro-thermal, electro-magnetic, Hall Effect and electro-static. Electro-static, also known as Kaufman, is perhaps the simplest and most elegant form. The propellant, either a gas or liquid, is fed into a chamber where it is ionised by electron bombardment creating a plasma of positively charged ions and electrons. The electrons are carried away by an anode and the ions are allowed to drift towards two accelerating grids. The grids have a potential of a few kilovolts across them and their small separation generates an extremely strong electric field. The ions are accelerated by the field and are expelled out of the spacecraft transferring momentum to the grids and generating thrust. The thrust is transferred to the spacecraft which is gently propelled. Technical issues greatly complicate the process but the basis principle is such.

3 Theory

Electrostatic propulsion works by accelerating a propellant through the application of electrical energy in the form of an electrostatic field.

Electrostatic propulsion can be divided into three main processes: Ion generation, ion acceleration and ion neutralisation. Ion generation is arguably the most difficult (and energy costly) of the processes and involves the generation of singly charged positive propellant ions. Three techniques are common: Thermionic electron bombardment, Caesium-Tungsten surface contact ionisation and RF discharge ionisation. Thermionic electron bombardment is the simplest method and has been chosen for this investigation.

The figure below shows a schematic of a simple electron bombardment electrostatic ion thruster (Kaufman ion thruster).



The gaseous propellant (often Xenon due to its inert properties) enters the ionisation chamber at low pressure where it is bombarded by low energy electrons. These electrons are emitted by a thermionic cathode (Hollow cathodes and Finite Element Arrays (FEAs) can also be used) in the centre of the chamber and are accelerated to the surrounding cylindrical anode by a positive potential difference. The potential difference is adjusted to give the electrons sufficient Kinetic Energy to ionise the neutral gas atoms leaving a positive plasma of propellant ions and electrons.

$$\text{K.E.} = eV$$

Where e = electron charge and V = potential difference.

1st Ionisation energy of Xe = 12.12 eV

1st Ionisation energy of N₂ = 14.54 eV

To extend the path length of the electrons and increase the ionisation probability a strong radial magnetic field is applied which exerts a Lorentz force:

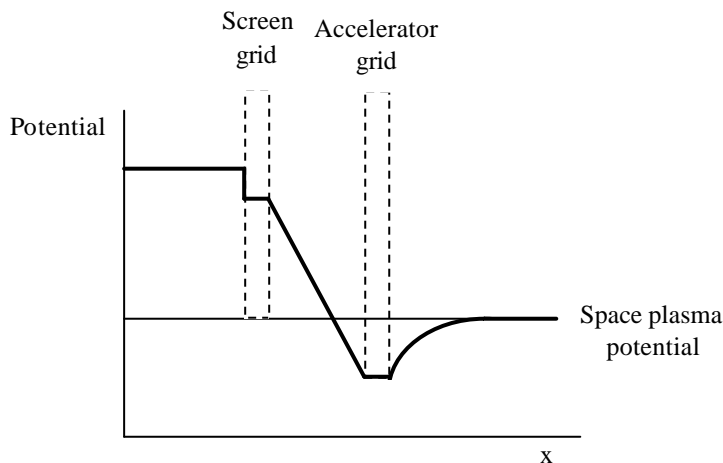
$$\underline{\mathbf{F}} = e(\underline{\mathbf{v}} \times \underline{\mathbf{B}})$$

Where \mathbf{B} = magnetic field and v = electron velocity.

This causes the electrons to spiral in the chamber at the Larmor radius, r :

$$r = \frac{vm}{eB} \tag{1}$$

before eventually being absorbed by the anode. The propellant ions also feel a Lorentz force from this magnetic field but because of their low q/m ratio they have a much larger radius and lower cyclotron frequency.



Further electrical Lorentz forces then cause the positive propellant ions to drift through the more negative screen grid where they are accelerated to extremely high velocities by an intense electric field from the negative potential of the accelerating grid. The ions exit the thruster through the accelerating grid

forming the ion beam. The thrust generated from the accelerated ions is exerted on the accelerating grids which is transferred through the thruster to the spacecraft.

The emission of such a large positive ion current would soon build up a positive space charge potential (negatively charging the entire spacecraft!) causing the beam to stall or reflect back on itself. To prevent this occurring a secondary thermionic cathode is positioned near the beam exit to inject electrons neutralising it. Although care must be taken to ensure a sufficiently high density of electrons are produced by the neutraliser that is the only precaution necessary as the electron/ion recombination process occurs efficiently and naturally on its own. The recombination/de-excitation processes cause the ion beam to pleasantly glow.

The exhaust velocity, u_i , of the ions is related to the q/m ratio and the accelerating potential:

$$eV = \frac{1}{2} m u_i^2 \quad (2)$$

$$u_i = \sqrt{\frac{2eV}{m_i}} \quad (3)$$

The thrust is therefore given by the product of exhaust velocity and the propellant mass flow rate:

$$F = (m u_i) = I \sqrt{2V m_i / e} \quad (4)$$

Where F = thrust, m = propellant mass flow rate, m_i = ion mass, u_i = exhaust velocity and V = accelerating potential.

A greater number of ions accelerated produces a greater thrust, however, ion thrusters are limited by a phenomenon known as “Space-charge”. If too many positive ions approach the accelerating grid their combined electric field can cancel the accelerating field, preventing the acceleration of further ions. This space-charge limit, the maximum ion density permitted in the thruster, can be calculated by applying Poisson’s equation, which is a generalisation of Coulomb’s law:

$$\nabla^2 V = 4\pi\rho \quad (5)$$

Where ρ = charge density = number of ions per unit volume between the accelerating grids and V = accelerating potential.

Substituting charge density using the relation, $J = v\rho$, where J = current density and v = average ion velocity, this becomes:

$$\nabla^2 V = 4\pi J/v$$

For flat grids this can be simplified with geometric assumptions to:

$$\nabla^2 V = \frac{d^2 V}{dx^2} = 4\mathbf{p} \frac{J}{v}$$

By substituting v with the expression for exhaust velocity from equation 3, this becomes:

$$\frac{d^2 V}{dx^2} = 4\mathbf{p} J \sqrt{\frac{m_i}{2eV}}$$

A solution for two plates separated by distance d can be shown as:

$$V = 9\mathbf{p} J d^2 \frac{m_i^{2/3}}{2e}$$

Thus maximum current density is given by Child's equation⁴:

$$J = \frac{1}{9\mathbf{p}} \frac{V^{3/2}}{d^2} \frac{2e}{m_i} \quad (6)$$

Equation 6 shows that current density and hence thrust are only dependent on the electric potential (accelerating potential) and the grid separation, provided sufficient ions can be generated. By increasing the accelerating potential or decreasing the grid separation the thrust can be increased, however, electrical breakdown between the grids puts an upper limit on this.

Space charge limitations put a theoretical upper limit on thrust density to a few Newtons/m² and so to generate higher thrusts a larger thruster diameter is required.

c.f. NASA's Deep Space 1 comet rendezvous mission was powered by a 30 cm diameter, 2 kW electron bombardment ion thruster with a specific Impulse of 3100 secs. It generated a beam current of 1.76 amps with a thrust of 92 mN but consumed only 12 kg of propellant during its entire mission.

From equation 3 it can be seen that exhaust velocity is only dependent on the q/m ratio and accelerating potential. Thus to increase the velocity lighter ions such as H₂ could be used.

In real case scenarios H_2 generates an exhaust velocity that is actually too fast for most space missions, creating a less desirable overall velocity increment. Reducing the accelerating field would reduce the exhaust velocity but it would also reduce the ion beam density and hence the thrust. Instead engineers opt to use ions with a lower q/m ratio such as caesium or mercury. Xenon is now more commonly used as the produced exhaust beam is inert minimising damage to spacecraft and thruster surfaces. It also requires less energy to ionise.

Thruster efficiency is an important property to be considered especially for long duration missions. The efficiency is the ratio of input energy to useful output energy. Ion thrusters typically perform at very high efficiencies which is one of their key advantages.

Electrical efficiency can be easily calculated:

$$\mathbf{h}_e = \frac{P_B}{P_{In}} = \frac{I_B V}{P_{In}} \quad (7)$$

Where η_e = thruster electrical efficiency, P_B = beam power, P_{In} = power in, I_B = beam current and V = accelerating potential.

However, to consider the overall thruster performance it is necessary to include the thruster's efficiency at converting propellant atoms into useful ions i.e. how much of the propellant mass flow actually contributes to thrust? This is known as the mass utilisation efficiency and is given by the ratio of the propellant mass ionised to the propellant mass flowing through the thruster:

$$\mathbf{h}_m = \frac{m^+}{m}$$

Where m = propellant mass flow rate and m^+ = ionised propellant mass flow rate.

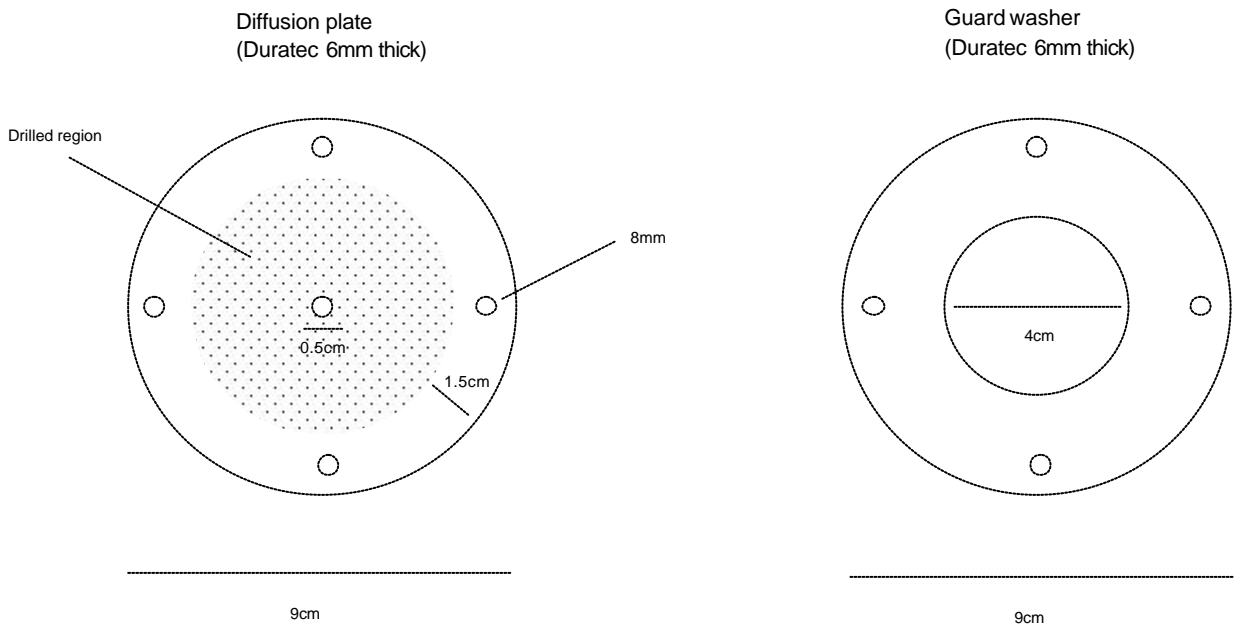
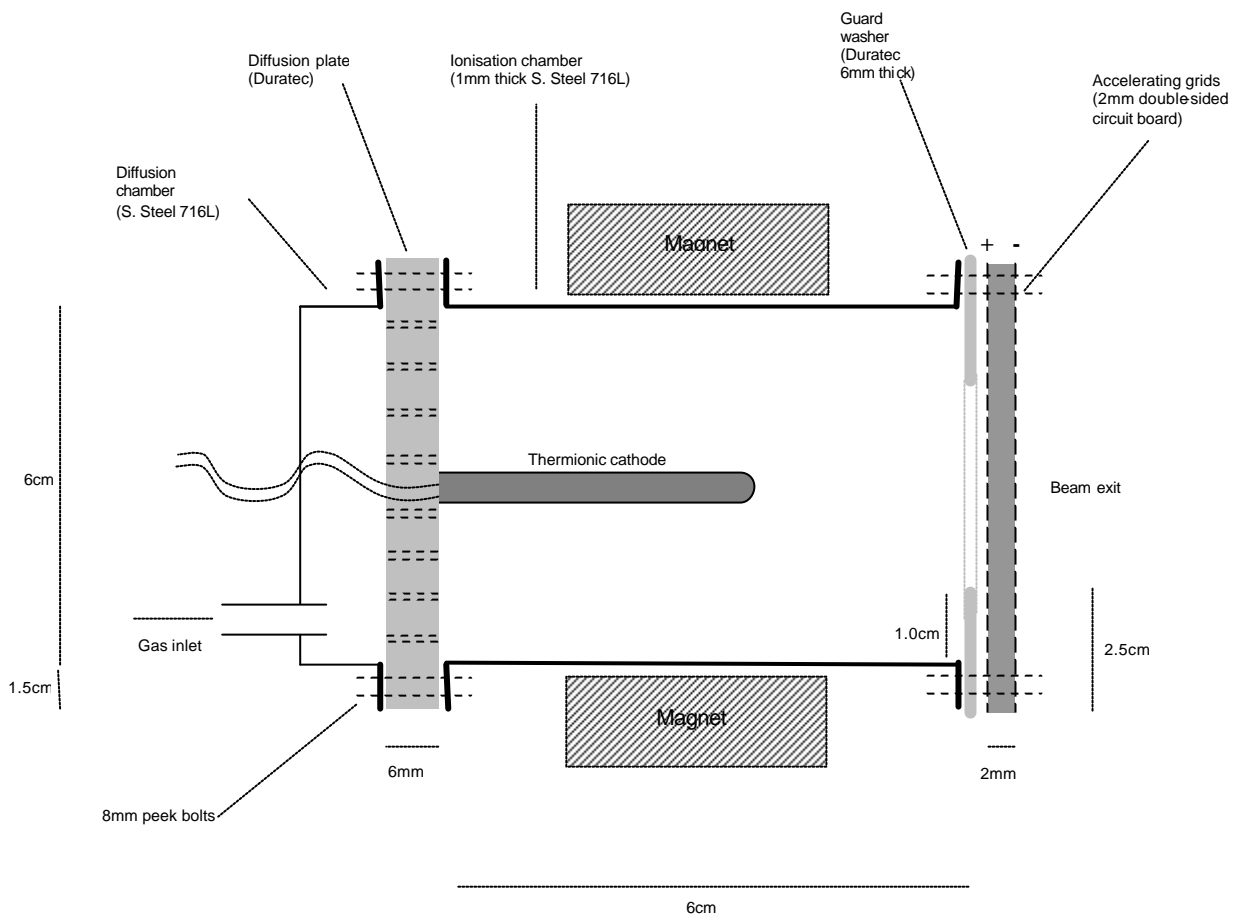
Thus the overall thruster efficiency, \mathbf{h}_t , is given by:

$$\mathbf{h}_t = \mathbf{h}_e \mathbf{h}_m \quad (8)$$

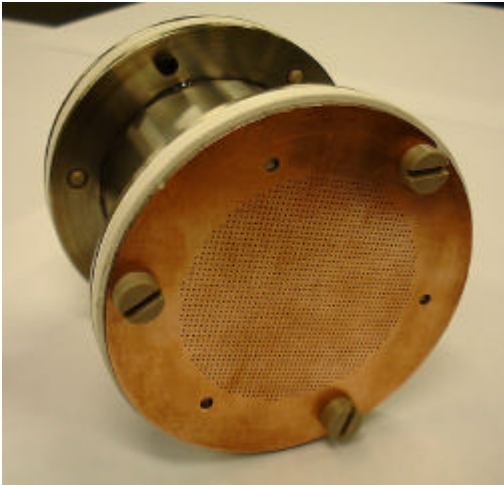
4 Design and Construction

4.1 Design Schematic

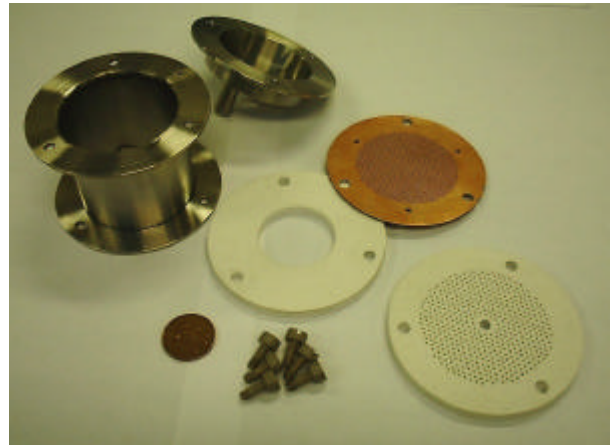
Below is the design schematic for the ion thruster as fabricated by the mechanical workshop.



4.2 Thruster design



(front view of assembled thruster)



(thruster components)

The thruster design is based on experimental and tested thrusters taking various design aspects from a multitude of configurations.

The main design requirement was to be adaptable and modular allowing a variety of configurations to be tested to allow an evolutionary research approach.

The main section is the ionisation chamber which doubles as the electron-source anode. It had to withstand high temperatures and ion/electron impingement and be a good electrical conductor. To maximise the magnetic field within the chamber from the externally placed magnets it must be non-magnetic. Aluminium was selected but due to a shortage the ionisation and diffusion chamber were made from Stainless Steel 316L. This grade of steel has one of the lowest magnetic characteristics and is very similar to aluminium.

The Diffusion plate and guard washer had to be electrically and thermally insulating while being able to resist potentially high temperatures from the thermionic cathode. They were produced from 'Duratec 750' which is made from calcium silicate. See appendix A2. To hold the sections together while maintaining electrical isolation 6 non-conducting, high temperature 'Peek' screws were specially created. See appendix A3.

Finally, the accelerating grids were constructed from double sided copper circuit board. The circuit board provided a rigid, fixed separation (2mm) between the grids and was easily machined. The board was double drilled to give larger diameter holes on the inside (screen grid)

and smaller on the outside (accelerator grid). The smaller open area of the screen grid helps to focus the ion beam and also reduces the loss of neutral propellant atoms from the ionisation chamber⁶.

4.3 Cathode arrangement

The nitrogen propellant ions are generated through bombardment by low velocity electrons in the ionisation chamber. The production of ions is the greatest energy cost of the thruster and so it is important that it is done as efficiently as possible. Careful choice of electron source was essential. There are many sources of electrons available. Typically electrostatic thrusters use a complicated 'Hollow cathode' arrangement but for simplicity and flexibility Thermionic emission was chosen for this investigation. Thermionic emission relies on the 'boiling-off' of electrons from an electrically heated material and subsequent acceleration through a positive potential difference.

i) Oxide coated filaments

One of the most recent advances in thermionic emission is that of oxide coated filaments. The oxides of Barium and strontium have work functions sufficiently low that they only require heating to 750°C before releasing electrons. A common technique used in many thermionic valves is to coat a Tungsten cathode with the oxide of Strontium or Barium. A separate tungsten heater is used to heat the oxide which releases a large number of electrons at a relatively low temperature. Tests on a GZ37 valve showed electron currents of several hundred milliamps could easily be produced.

Such a rectifier valve was broken open and the cathode was mounted onto the diffusion plate using 'Fire cement' which is non-conducting and can withstand temperatures of up to 2000°C. Unfortunately, it was later found that the oxide coating decomposes in air to form the useless hydroxide⁷ and no electrons could be produced using this set-up.

ii) Tungsten/Thorium alloy

By using an alloy of tungsten and thorium the work function of the material is greatly reduced and will emit electrons when heated to only 1600°C. Unfortunately this alloy was unavailable for the project.

iii) Direct thermionic emission

By heating a material to $>2000^{\circ}\text{C}$ the electrons are given sufficient energy to break free and as free electrons. The temperature of electron emission depends on the work function of the material. A common material used, due to its ability to withstand high temperatures, is tungsten which must be heated to approximately 2200°C to release electrons.

According to the Fermi-Dirac distribution the released electron current flow coming from the surface of any solid is given by the Richardson-Dushman equation⁸:

$$j = \frac{4pm_e}{h^3} k^2 T^2 \exp\left[\frac{-ef}{kT}\right]$$

Where j = electron current density, m_e = electron rest mass, f = work function, T = temperature and k = Boltzmann's constant.

Low power torch light bulb filaments (tungsten) were tested and found to initially produce a large electron current which quickly diminished to zero over a period of about 20 mins. This was later found to be due to the evaporation of the tungsten from the filament, accelerated by the high vacuum environment.

A higher power bulb filament was tested whose larger filament area meant a lower operating temperature was needed to produce the same electron current. This reduced the tungsten evaporation rate and provided a stable electron source.

The electron current was found, however, to vary considerably with time requiring constant re-adjustment of the power input. The larger filament also required significantly more energy and created a greater heating effect of the thruster body as a whole. The low Curie temperature (80°C) of the NdFeB magnets meant this heating effect could be a problem and had to be further investigated.

An attempt was made using an optical pyrometer to measure the filament temperature to compare with the Richardson-Dushman equation. Unfortunately, the vacuum dome made measurements difficult and the results questionable.

5 Magnetic containment

The production of positive propellant ions is the most energy depleting process and so it is of vital importance that it is done as efficiently as possible. The energy cost per ion produced must be kept to a minimum and so it is desirable that the ionisation probability from an electron emitted by the cathode is maximised.

By applying a strong axial magnetic field the electrons experience a Lorentz force:

$$\underline{\mathbf{F}} = e(\underline{\mathbf{v}} \times \underline{\mathbf{B}})$$

Where \mathbf{B} = magnetic field, e = electron charge and v = electron velocity.

This force causes the electrons to spiral about the cathode before being absorbed by the positive ionisation chamber walls (anode). This spiralling increases their path length and hence time of flight which increases their probability of colliding with a propellant atom. The Lorentz force is perpendicular to the magnetic field direction and has no effect on the electron velocity. The electrons spiral in a plane although suffer slight axial drift due to electrical forces from the screen grid.^a

The applied magnetic field can also have complicated effects on the ion beam emerging from the rear of the thruster although, for this investigation these effects have been ignored.

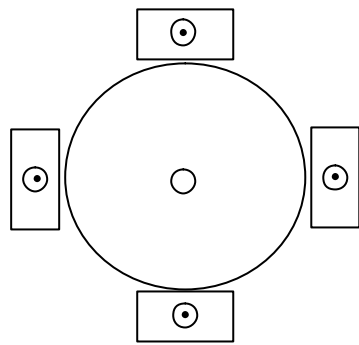
5.1 Magnet orientation

The divergent axial magnetic field is a common orientation and was chosen for this investigation.

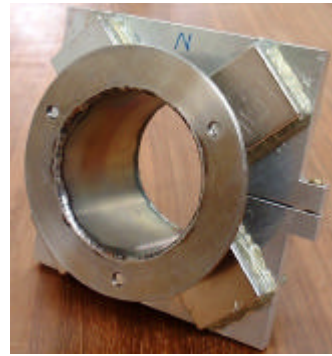
The magnetic field was provided by four 29x30x25 mm NdFeB (Neodymium-Iron-Boron) grade 42 rare earth magnets. NdFeB was discovered in the 1980s and is the strongest permanent magnet known. See Appendix A4 for more information.

Ideally a circular ring magnet placed around the ionisation chamber would provide a perfectly symmetric field but 4 adjacent block magnets make a good approximation. The magnets were mounted into a non-magnetic removable jig to hold them in place, exactly 90° apart. See picture below.

^a The effect of the magnetic field from the current flowing in the cathode has been ignored.



Axial view of thruster showing magnet orientation and field direction



Magnet jig around ionisation chamber

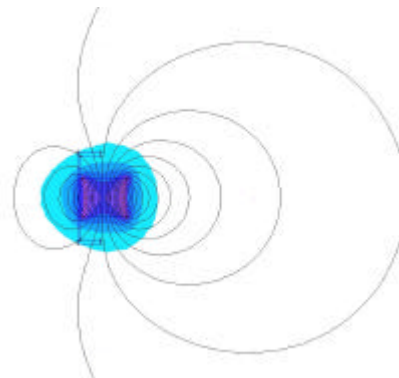
5.2 Femme Modelling

To calculate the magnetic field inside the ionisation chamber an advanced computer modelling program called Femme (Finite Element Method Magnetics) was used. The program is able to solve static two-dimensional axisymmetric problems by breaking the domains down into small finite elements and then solving the relevant Maxwell equations for these simpler geometric shapes. By using computer intensive algorithms these finite regions can be combined to produce a solution for the whole domain. More information can be found from the Femme website⁹ where the program can be freely downloaded.

The thruster design was inputted into the program as a side view to calculate the magnetic field strength and geometry inside the ionisation chamber. All thruster dimensions and materials were entered accurately to allow the correct field geometry to be calculated. As the program deals only with axisymmetric problems the magnets were simplified to a ring magnet around the circumference of the chamber. The problem geometry is shown below together with the magnetic field solution:



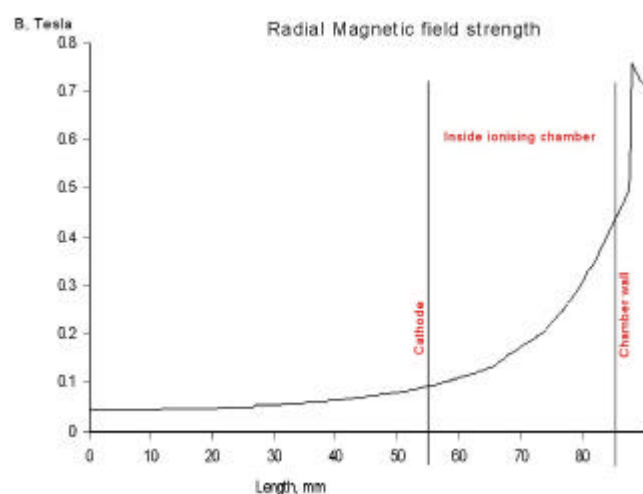
*Half-cylinder cross section
(Femme Model)*



Magnetic field solution

As you can see the majority of the field is on the outside of the chamber with only a few flux lines permeating the centre of the chamber. The field within the chamber is symmetric simplifying calculations. The colours represent flux intensity. A larger version of this diagram including the legend is given in appendix A6.

The graph below shows the magnetic field strength against radial distance for the centre of the chamber (as calculated by Femme):



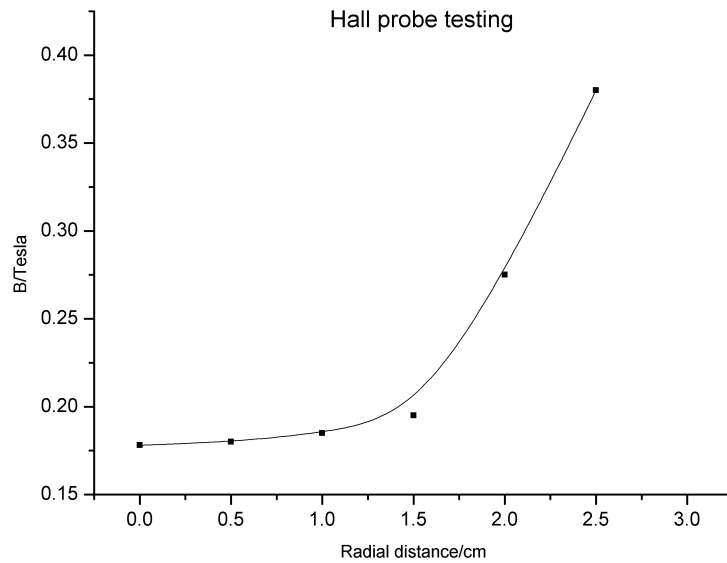
From this graph it can be seen that the field strength at the centre of the chamber (cathode) is predicted to equal roughly 0.09 Tesla increasing to 0.45 Tesla at the chamber walls (anode).

Using the graphing program ‘Origin’ the equation of this curve was found using a polynomial Sigmoidal fit. The equation of the curve was found to be: $y = 0.085 - 0.0045x + 8.92x^2$. See appendix A7.

5.3 Hall probe verification

To determine the accuracy of the Femme model, remembering the assumption of the ring magnet made, a Hall probe was used to determine the actual field strength within the ionisation chamber. A grid was produced, divided into angular divisions of 22.5° and radial distance divisions of 0.5 cm, to aid in the measurement of the centre planar radial magnetic field. A “Scientifica and Cook Electronics” Hall probe was used with an accuracy of $\pm 2\%$. The radial field was plotted below. The error bars indicate the $\pm 2\%$ accuracy of the probe but not the error in positioning the probe which is estimated to be ± 1 mm. The probe used was 9 mm wide and so it was very

difficult to obtain a wide range of radial measurements. The width of the probe also makes the chamber wall measurements difficult to obtain producing a higher uncertainty.



The graph shows that the actual field looks roughly of the same form and magnitude as that predicted by Femme. A larger number of data points would improve the fit. Field strength at the centre of the chamber (cathode) was found to equal 0.178 Tesla increasing to 0.40 Tesla at the chamber walls (anode). The field at the centre is higher than that predicted by Femme.

The magnetic field was found, for the most part, to be symmetric.

Using equation 1 the electron Larmor radius for the centre of the chamber can be calculated:

$$r = \frac{vm}{eB} = \mathbf{0.19 \text{ mm}}$$
 (assuming a potential difference of 100 V)

Where v = velocity, m = electron mass, e = electron charge and B = magnetic field strength.

5.4 Fortran Modelling

The magnetic field within the ionisation chamber is non-uniform and so it is quite complicated to model the trajectory of the emitted electrons. It is necessary to solve the two equations of motion for the electrons in a magnetic field which are second order coupled differential equations:

$$F = ma = e(\mathbf{V} \times \mathbf{B})$$

$$\Rightarrow \mathbf{a}(x,y) = e/m(\mathbf{V}(x,y) \times \mathbf{B}(x,y))$$

Splitting into components:

$$\ddot{x} = \frac{e}{m} \bar{B}(x, y) \dot{y} \quad \ddot{y} = -\frac{e}{m} \bar{B}(x, y) \dot{x}$$

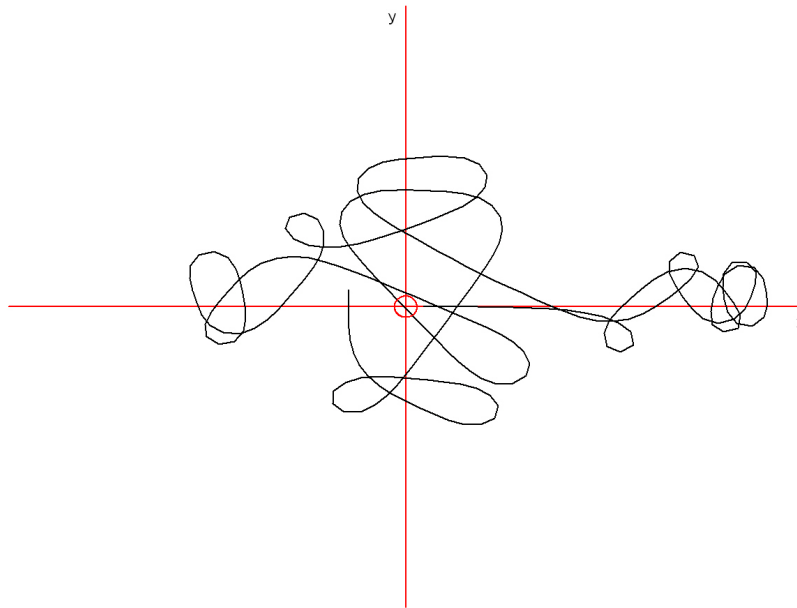
The Gear-Nordsieck method is a sophisticated ‘predictor-corrector’ method for solving such equations and can be run as a subroutine through a FORTRAN computer program.

A suitable program to call this subroutine was written and the trajectory of the electrons plotted.

The Femme prediction was used as the model for the magnetic field.

The listing for the program is given in appendix A8.

A plot of the possible trajectory of an emitted electron within the ionisation chamber is given below. The cathode is at the centre; the chamber walls are not shown.



As you can see the path is completely random – a result of the non-uniform magnetic field. Despite the un-predictability of the particle, the path length is enormously increased which greatly increases the particle’s chance of collision with a nitrogen molecule.

N.B. The model assumes the emission of a single electron into a complete vacuum experiencing no other interactions.

6 Optimal thruster configuration

As discussed earlier the maximum thrust of an ion thruster is limited by space charge effects which determine the maximum charge density that can be accommodated by the accelerating grids. By using Child's law (equation 6) and assuming an accelerating potential of 1000 V this maximum current density can be calculated:

$$\text{Maximum current density} = J = \frac{1}{9\epsilon_0} \frac{V^{3/2}}{d^2} \frac{2e}{m_i} = \mathbf{11.47 \text{ mA/cm}^2}$$

Where J = current density, V = accelerating potential (1000 V), d = grid separation (2 mm), m = nitrogen ion mass and e = electron charge.

$$\text{Maximum total current} = J \times \text{grid area} = \mathbf{144.14 \text{ mA}}$$

This total current represents both the maximum possible thruster beam current and the maximum electron current necessary from the cathode. Any additional electrons above this would generate an excess of propellant ions causing a total charge in excess of the Space-charge limit that would reduce the performance of the thruster. This assumes every emitted (primary) electron produces one propellant ion, ignoring any effect from 'knocked-off' secondary electrons. In actual fact the primary electrons contribute only a small fraction of the ionisation of the propellant, the majority is due to secondary electrons.

From this and using equation 4 the maximum possible thrust can be calculated:

$$F = I \sqrt{2V m_i / e} = \mathbf{3.48 \text{ mN}}$$

Where F = thrust and m_i = nitrogen ion mass. The actual thrust produced will not be anywhere near this value as losses will occur from a variety of factors including non-uniformities of the electric field between the grids, inelastic collisions of ions, ion impingement on the accelerating grids and ion vector divergence present in beam spreading. This last loss is caused by a radial spreading of the ion exhaust beam caused by the internal geometry of the thruster and from repulsive electrostatic forces between ions. It results in a non-axial beam velocity and a corresponding reduction in thrust.

The guard washer will help to minimise axial beam divergence by restricting the exit aperture but its main purpose is to improve beam flatness. Beam flatness is a measure of the radial distribution of the ion beam from the accelerating grid. Most thrusters produce a non-uniform beam distribution, strongest at the centre of the grid. The guard washer will block the grid aperture at the extremities reducing the loss of neutral propellant.

Assuming complete conversion of potential energy to kinetic energy the maximum beam power can be calculated:

$$P = \frac{1}{2}mv^2 = \frac{1}{2} \frac{Im_i}{e} \cdot \frac{2Ve}{m_i} = IV = \mathbf{144.14 \text{ Watts}}$$

Where m = propellant mass flow rate, m_i = ion mass, V = accelerating potential, I = current and e = electron charge.

Exhaust velocity can be calculated from equation 3:

$$u_i = \sqrt{\frac{2eV}{m_i}} = \mathbf{82.73 \text{ km/sec}}$$

Giving a maximum specific impulse, $I_{sp} = u_i/g = \mathbf{8433 \text{ secs}}$

Finally, the maximum propellant mass flow (the maximum quantity of nitrogen needed to be fed through) can be found from:

$$m = F/u_i = \mathbf{4.21 \times 10^{-8} \text{ kg/sec}}$$

These theoretical quantities provide the initial operating parameters for testing the thruster and predicting its behaviour.

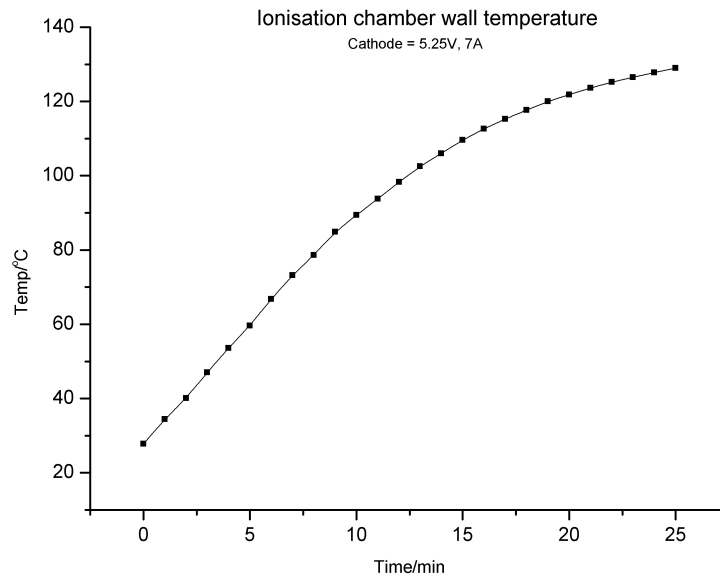
7 Temperature testing

A thermocouple was used to monitor the heating effect of the filament electron source to prevent overheating of the NdFeB magnets which lose their magnetism (non-permanently) at their Curie temperature of 80°C.

A J-type thermocouple was soldered to the centre of the outside of the ionisation chamber and the filament run at a fixed voltage and current of 5.25 V, 7 Amps for 25 mins.

The thermocouple was connected to an 'Analogue Devices' AD594 amplifier which had been previously calibrated. See Appendix A5 for calibration curve and further details.

The graph below shows how the temperature varies with time.



N.B. The thermocouple has an accuracy of $\pm 3^{\circ}\text{C}$. No propellant gas was flowing during the test which would normally have a slight cooling effect.

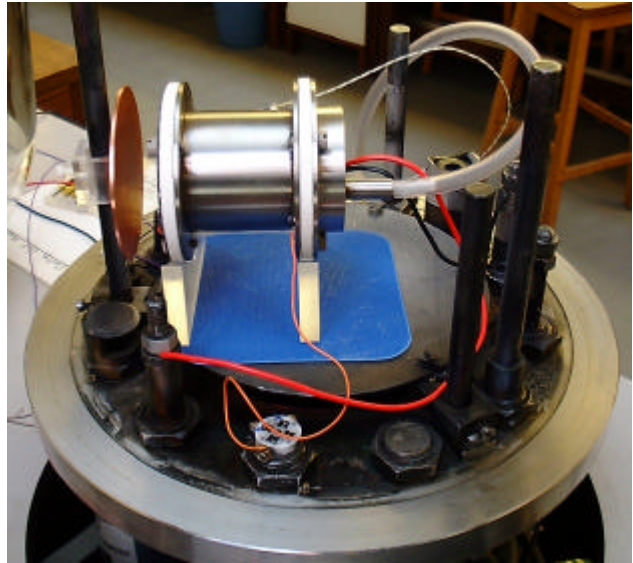
The test showed that the filament causes a serious heating problem that could cause the magnets to de-magnetise after only 8 minutes of operation.

To prevent this the ionisation chamber was wrapped in thick cotton to insulate and test runs limited to 15 minutes per session with a suitable break for cooling.

8 Experimental procedure



Edwards vacuum coating unit



Thruster arrangement

The experimental procedure was carried out in the Edwards vacuum coating unit E12E in the Part II lab. The unit has a large vacuum volume, a gas inlet feed and multiple electrical throughputs including high tension and high current. The combined rotary and diffusion pumps can produce a vacuum of micro-Torr magnitude. Conveniently it also has a glass dome allowing observation of the plasma exhaust. See appendix A1 for the pump-down procedure and schematic of the vacuum coating unit.

The thruster arrangement is shown in the picture above. Low oxygen nitrogen gas was used as the propellant from a compressed gas cylinder. No suitable gas control valve was available so the propellant flow was controlled directly using the needle valve on the front of the coating unit.

The limited space available in the vacuum dome prevented any accurate measurement of the thrust produced and so a copper plate was used to act as a Faraday collector. The plate was positioned in front of the accelerating grids to collect the emitted high velocity positive ions. The plate was earthed and an ammeter used to measure the current flow which corresponded to the emitted beam current. A neutraliser cathode to emit electrons and neutralise the ion beam was not used and so it was important to position the plate close to the beam exit to draw off the ions before they could be back accelerated to the accelerating grids.

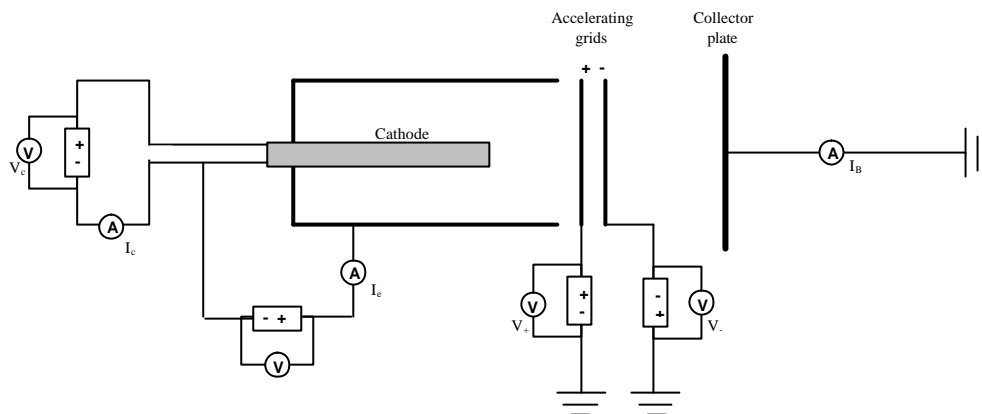
All components including the thruster itself were electrically insulated from the vacuum chamber, the inside of which was sprayed with an anti-corona coating to prevent discharges to

earth through the vacuum unit itself. Initially a thermocouple was soldered to the centre of the ionisation chamber to monitor the chamber temperature to prevent the magnets overheating.

All tests were carried out at 1.0 - 10 micro-Torr depending on the propellant flow rate.

The accelerating grid made from a double sided circuit board was found to be ineffective because of the small open area fraction and so a stainless steel gauze was used in its place.

Separate power supplies were used to power the electron-source filament, the electron source accelerating potential, the screen grid potential and the accelerating grid potential. The electrical configuration is shown below:



The Faraday current produced in the collector is directly proportional to the thrust generated and can be used as an indicator of the thruster's performance. From equation 4:

$$F = (m u_i) = I_B \sqrt{2V m_i / e}$$

Where F = thrust, m = mass flow rate, u_i = exhaust velocity, I_B = beam current, V = accelerating potential, m_i = ion mass (nitrogen ~4.68x10⁻²⁶ Kg) and e = electron charge.

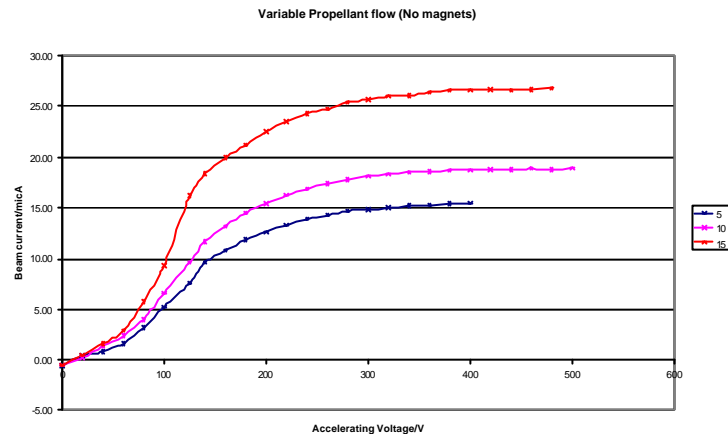
A series of tests were conducted to investigate the factors affecting the thrust produced by measuring the beam current produced for varying accelerating potentials. Factors investigated include electron discharge voltage and current, magnetic field strength within the ionisation chamber, accelerating grid geometry and grid sizing, and collector plate distance.

9 Results

Please note that full page versions of all the graphs can be found in the appendix together with the numerical results.

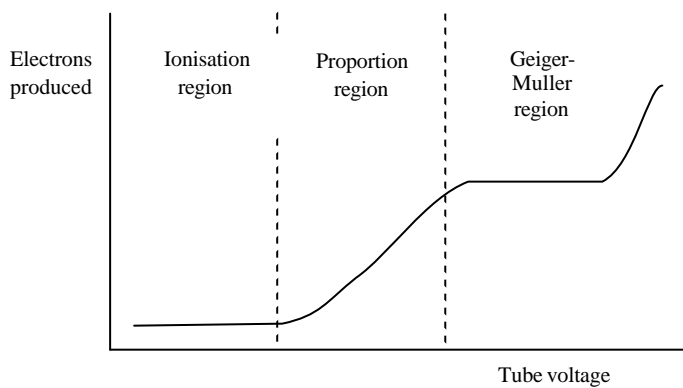
9.1 No magnetic field

The first sets of experiments were to determine the characteristics and accelerating performance of the thruster without any magnetic field. Propellant flow rate, discharge voltage and discharge current were varied to determine their effect. The results from this would then be used to plan further investigations. In this configuration the thruster was expected to perform unimpressively accelerating only a small fraction of the gas molecules.



Propellant flow: The graph above shows the beam current (indicative of thrust) measured from the collector plate against the increasing negative potential of the accelerating grid for varying propellant flow rates (increasing in units according to the needle valve). As you can see a higher beam current is produced for higher propellant flow rates. This is because at any one time there are a more nitrogen molecules present in the chamber and so the ionisation probability increases resulting in more charged ions that can be accelerated. It would be expected that further increases in propellant flow would eventually cause the beam current to decrease. This is because the gas density would become too high and inelastic collisions would become dominate to elastic ionisation collisions. This would reduce the number of charged ions in the chamber and hence reduce the beam current. Instead the thruster would spew excited (but uncharged) nitrogen molecules unaffected by the accelerating grid and hence not contributing any thrust.

As you can see from the graph the curve for beam current against accelerating voltage is not a linear relationship but more of a sigmoidal curve. The shape of this curve is thought to be due to the effect of the electric field on the ionisation process. The best way to explain the effect is by the example of a gas-filled radiation counter such as a Geiger-Müller tube. This consists of a metal tube filled with a low pressure gas with a wire running down the centre. There is a high potential difference between the central wire and outer tube creating a strong electric field. As a high energy particle traverses the tube some gas molecules become ionised. The electric field causes charge separation in which positive ions are accelerated to the cathode and the negative electrons are accelerated to the anode where they register as a current in an external circuit. The charge separation and ionisation process is dependent upon the gas pressure and applied accelerating voltage. The response curve is shown below:



There are three distinct operating regions of the detector. In the ionisation region the accelerating voltage is low and the number of electrons produced is equal to the number of electrons/ions produced by the incident charged particle. In the second region, however, the accelerating potential is strong enough for the

produced electrons to gain enough energy from the electric field to cause secondary ionisation from collisions with gas molecules. This process is called gas multiplication. The number of electrons produced is proportional to the number of primary ion pairs produced by the incident particle and so the region is called the proportional region. If the accelerating voltage is increased further the Geiger-Müller region is reached. Here the number of electrons produced becomes independent of the number of primary ion pairs produced. Each ionising event causes a discharge which fills the chamber and the total discharge is limited only by the characteristics of the chamber and counter gas, saturation occurs.

If the accelerating voltage is increased beyond this region no ionising event is required to create a continuous discharge – it is generated by random free electrons in the chamber.

The ion thruster suffers a similar process only more complicated because of the two electric fields (one field to accelerate the electrons causing ionisation of the gas and a stronger field to accelerate the positive ions out of the thruster). The graphs clearly show that as the accelerating

field is increased gas multiplication is occurring that is causing a proportional increase in the number of ions produced. The multiplication effect is likely to be caused from the repulsion of the electrons from the accelerating grid rather than the attraction of the ions which are heavier and move more slowly (initially). The curve eventually flattens out whereby any further increases in the accelerating field do not cause further increases in particle ionisation. The chamber has become saturated and any further increases in beam current can only be brought about by additional factors such as propellant flow rate etc.

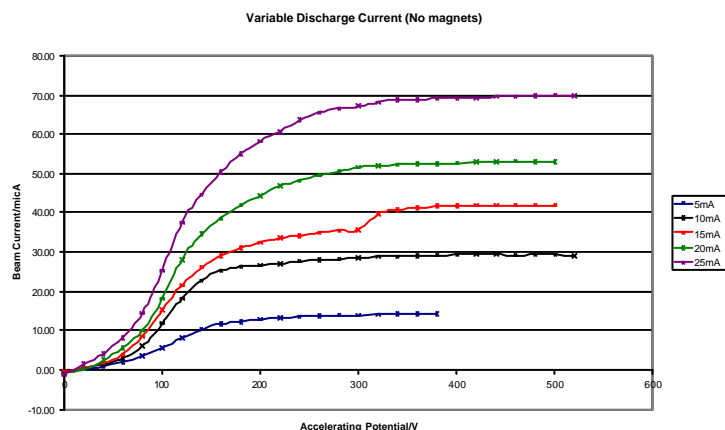
Continuous discharge observation

It was noted during initial testing that in some circumstances a significant beam current was produced without the electron source filament being switched on i.e. the neutral gas molecules were somehow ionising themselves enabling them to be accelerated through the grid. This occurred at very high potentials and high pressures ~1 mTorr (far too high for effective ion thruster operation). This was a puzzling situation but can now be accounted for with the gas-filled counter theory: The high pressure and accelerating voltage (in excess of the Geiger-Müller limit) meant that random free electrons were able to create a continuous discharge within the chamber resulting in the produced beam current detected.

Using this property and assuming no energy losses from ions impinging on the accelerating grids it is possible for such a device to generate thrust without expending any energy! The thruster would, however, be very wasteful of propellant with the majority of the gas particles leaving the thruster uncharged and un-accelerated.

Discharge Current

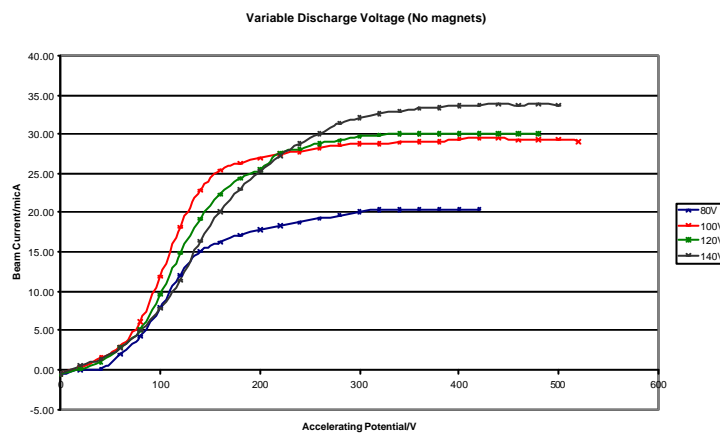
By increasing the filament input current it was possible to generate a larger number of electrons in the chamber without increasing their energy (constant discharge voltage).



The graph above shows the effect of increasing the discharge current for a fixed discharge voltage. As you can see the beam current is highly dependent upon discharge current and increases roughly linearly to it. This is because at higher discharge currents there are more electrons within the chamber increasing the ionisation probability. You may think it prudent, in order to maximise the output of the thruster, to increase the discharge current to a very high value flooding the chamber with electrons. However, this increases the inelastic scattering rate but more crucially increases the power input resulting in a decrease in overall efficiency. As with many factors affecting the performance of an ion thruster an operational balance must be found between input energy and output thrust.

Discharge voltage

Finally the electron accelerating field (discharge voltage) was varied. It is essential for the primary electrons to have sufficient K.E. to ionise the nitrogen molecules, whose first ionisation energy is 14.5 eV (equivalent to a potential of 14.5 V). It is advantageous to have a higher potential, however, as more electrons can be drawn from the source, the secondary electrons can be accelerated to a sufficiently high energy to create secondary ionisation and the chances of inelastic collisions are reduced. The graph below shows the beam current for varying discharge voltages.



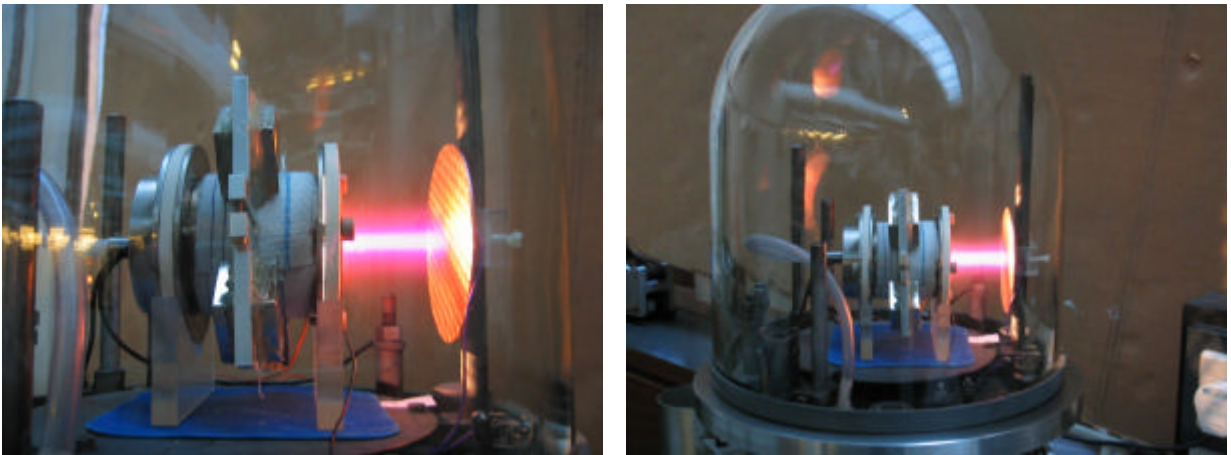
It is possible to observe from the graph that there is a threshold voltage for which the generation of nitrogen ions becomes efficient but also there is a limit for which further increases in voltage do not cause any significant increase in ion production. This limit is likely to be where the electric field is strong enough to allow secondary electrons to cause secondary ionisation – any further increases of voltage would therefore have little effect.

9.2 Full magnetic field (4 magnets)

The next sets of experiments were to determine the effect of a strong axial magnetic field on the performance of the thruster. As shown in section 5.4 an axially applied magnetic field can dramatically increase the path length of the primary electrons, greatly increasing their probability of collision and ionisation. It was expected that the use of magnets would completely change the performance characteristics of the thruster and greatly increase the produced beam current. The four NdFeB magnets were attached to the thruster using the jig shown in section 5.1.

Plasma discharge observation

Almost immediately after the thruster was initialised and the discharge current increased a bright plasma emission was seen emanating from the accelerating grid to the collector plate. See pictures below:



Thruster plasma discharge

The bright exhaust plume visible is caused mostly from the natural drift of propellant gas out of the thruster. The nitrogen atoms are in an excited state from inelastic collisions within the ionisation chamber and as the electrons return to their ground energy state they release energy as photons. These photons are of a characteristic frequency corresponding to nitrogen – as you can see it is a pinky/reddish colour.

The emission of light from ion thruster exhaust plumes is a general characteristic however it is normally caused by the re-combination process of positive propellant ions and neutraliser electrons from a second external electron source. No neutraliser was used in my setup and so the light is due to de-excitation of excited, but uncharged and un-accelerated propellant ions. The

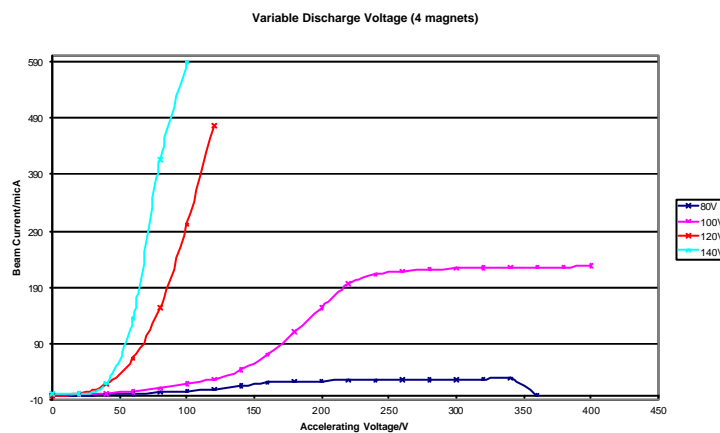
emission of light represents a loss of propellant from my thruster and its brightness most likely indicates that the propellant flow rate is far too high.

As discussed earlier the number of inelastic collisions is related to the gas pressure within the chamber, an increase in pressure would result in more collisions, producing more excited atoms and hence more light. The flow rate was increased and as predicted the light intensity increased.

It was also noted that in order for the plasma emission to initiate the discharge voltage had to be raised to a high level ($>110\text{V}$). Once initiated, the plasma discharge became self-sustaining and the discharge voltage could be reduced to lower values. This is a result of the gas multiplication effect and is common in plasma experiments.

Discharge voltage

Again the discharge voltage was varied to determine its effect and as expected the presence of a magnetic field markedly affected the behaviour of the thruster. The presence of the magnetic field increased the beam current in all cases and is solely due to the increased ionisation probability due to the increased path length of the electrons.

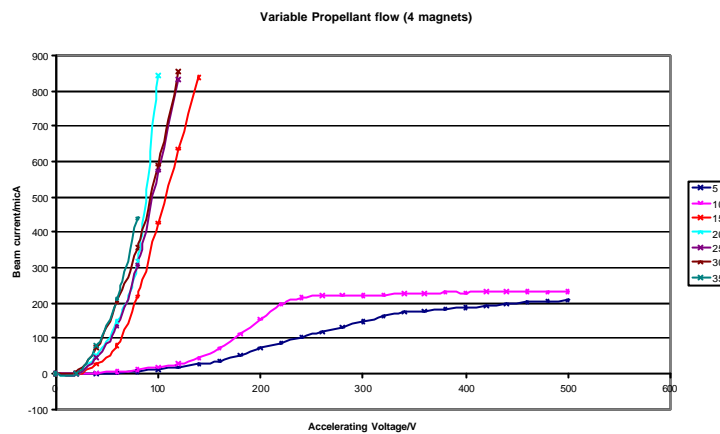


As before there is a clear discharge voltage threshold for which the ionisation process becomes effective. Below this threshold the secondary electrons do not have enough energy to ionise nitrogen atoms and so the number of ions created is limited, eventually a maximum is reached and the curve flattens off. Above this threshold, however, the secondary electrons are able to ionise and gas multiplication occurs. The vast numbers of secondary electrons become the dominant ionising agent. The magnetic field causes the electrons to linger and randomly circulate within the chamber ionising further atoms. This causes a surge of ions and hence a massive increase in ion current. It was not possible to take further readings because the low-

current accelerating-voltage power supply was struggling to cope with the current generated from ion impingement on the accelerating grid. This impingement represents a serious loss of ions from the beam and also a significant power drain.

Propellant flow

The effect of propellant flow rate was investigated and again it was found that this was a critical factor affecting performance.



The graph clearly shows that again there is a threshold flow rate for which ion production becomes efficient. At lower flow rates the gas pressure is too low for gas multiplication to occur – the particles are simply too far apart. Once above this limit further increases in flow rate do not significantly affect the beam current. It can be seen that beam currents approaching 1 mA could now be achieved – far higher than could be produced without the magnetic field.

9.3 Fine mesh accelerating grid

To determine the effect of the accelerating grid spacing a finer grid was tested, again made from stainless steel but with finer mesh and smaller holes.

See appendix for results and graphs.

The finer grid produced far higher beam current values but unsurprisingly suffered greater ion impingement. The resulting current produced in the grid limited the performance of the power supply and so it was only possible to take a few readings. It was estimated that the current produced in the accelerating grid was 120% of the beam current – an appalling figure for any ion thruster.

9.4 Effect of collector distance

To determine if the strong electric field from the accelerating grid produced any effect on the current produced in the collector plate, the distance from the beam exit to the collector was varied. See appendix for results.

No clear relationship could be determined. Repeat readings at smaller distance intervals may provide clearer results.

9.5 Reduced magnetic field (2 magnets)

From my calculations for the Larmor radius of the electrons at the centre of the chamber (section 6.3) it was thought that the magnetic field was too strong and caused the emitted electrons to circulate in a small region at the very centre of the chamber. This would mean that the propellant ions would only be ionised in this region producing a very narrow beam (low beam flatness). This was confirmed by the erosion pattern on the collector plate (see later) which showed the majority of erosion occurred in one central spot.

This low beam flatness means that a large area of the accelerating grid was not being used and as thrust is proportional to the grid area, reduces the thruster's effectiveness.

By reducing the magnetic field strength the electrons would be able to circulate in a larger region of the chamber creating more ionisation at the extremities and a flatter beam. This should produce beam current values far higher than before. To test this, two adjacent magnets were removed from the jig and the tests re-run.

See appendix for graphs.

The results show that using two magnets produces higher beam current values than that for no magnetic field but the values were far lower than that for 4-magnets. This may be because the field was simply not strong enough or that using 2 magnets 180 degrees apart creates a non-symmetric field that is not suitable for electron containment. A hall-probe survey could be used to determine the field strength/symmetry within the chamber.

It is clear, however, that the magnetic field strength is a trade-off: it must be strong enough to contain the electrons in the chamber but not too strong to limit their motion to a small region.

9.6 Multiple accelerating grid arrangements

Ion thrusters typically have two or more accelerating grids. As was to be the case for my original design, there is usually a less positive (compared to the ionising anode potential) screen grid that acts to focus the ions followed by the main accelerating grid. For simplicity my thruster was operated using a single accelerating grid but a multiple grid arrangement was tested.

Despite various applied potentials the screen grid's only affect was to actually reduce the beam current. In order for the focussing property to become effective both the screen grid and accelerating grid must be perfectly aligned. This was probably not the case and so resulted in a decrease in beam current and an increase in ion impingement.

What was found more effective, however, was the use of two parallel, negative accelerating grids of similar potential. The effect was to produce double the beam current.

Effectively the ions experience twice the accelerating force producing a higher beam current.

Ion impingement, equally on both the grids, was still a problem however. The results of the maximum produced beam current are given below:

Grid 1: Potential = -98 V, grid impingement current = 1.161 mA

Grid 2: Potential = -92 V, grid impingement current = 1.196 mA

Beam current = 2.33 mA

Using equation 4 the thrust can be calculated:

$$F = (mu_i) = I\sqrt{2V m_i/e} \quad (4)$$

Maximum produced thrust = 0.03 mN

10 Sources of error

For such a complex investigation the sources of error in the experimental procedure are varied and numerous.

The multimeters used for measuring the electrical properties have an accuracy of $\pm 0.5\%$ for current and voltage and the power supply readings have an error proportional to the resolution of the dials.

The Penning/Pirani pressure gauges on the Edwards evaporator have not been calibrated in a long time and so all pressure measurements can only be used as a rough guide. Unfortunately there was no way to verify their accuracy.

Although the Faraday collector plate is used to measure the beam current it is possible that a large proportion of the high energy positive ions (of energy upto 1000 eV) are not collected by the plate but are either back-scattered (in a process similar to electron back-scattering from atomic nuclei) or collide with the copper atoms of the collector surface creating secondary ionisation or a shower of secondary particles. The collector surface shows clear signs of particle erosion (see picture) indicating a loss of material. In the centre of the plate a pattern matching that of the square grid arrangement is clearly visible.



Collector plate erosion

These losses can be minimised by altering the geometry of the collector plate, however, it is a very technical problem to solve and is beyond the scope of this project. Although, varying the collector geometry was planned there was insufficient time to complete it.

A further error was generated by irregularities of the electron generation filament. It was noted that the electron current produced was not constant and tended to decrease over time (for fixed input power and accelerating voltage). This is thought to be caused by a gradual reduction in filament surface area caused by evaporation of the tungsten material accelerated by the

vacuum. The sporadic variations may be caused by the release of gases/ions adsorbed onto the filament surface.

By far the largest uncertainty however was caused by the input of propellant gas into the thruster. The extremely low volumes of gas used meant there was no way to measure the flow rate into the thruster. This means that it is not possible to determine the thruster's mass utilisation efficiency (how much input propellant was being converted into thrust) and hence the overall efficiency.

The gas flow was controlled using the needle valve on the front of the evaporator allowing the flow to be controlled according to the scale on the valve. It was assumed that the valve produced a linear increase in gas flow but there was no way to verify this. It was also noted that the valve control had suffered from wear and tear over the years and slight pressure applied while turning the valve could affect the flow rate. This is a huge cause for concern for the reliability of my data as it has been shown that the performance of the thruster is highly dependent upon the propellant flow rate. In any further investigation of this kind the accurate control and measurement of propellant flow would have to be a priority to be addressed.

11 Conclusions

The maximum thrust that was achieved was 0.03 mN, far lower than the theoretical maximum of the thruster design. A significant amount of current was lost by impingement on the grids and as shown by the emission of light a large amount of propellant was left uncharged and hence wasted.

My investigation has shown that it is relatively easy to generate thrust from the electrostatic acceleration of a propellant but it is far harder to generate a high thrust at high efficiency. Performance of electrostatic ion thrusters is dependent on a complex range of interdependent variables, mostly dominated by propellant flow rate, electron containment (and hence magnetic field strength and orientation) and also the electron discharge current and voltage.

My thruster design was limited by poor 'geometry' that led to a low ionisation probability and high ion impingement on the accelerating grids. Not only did this result in a loss of charged particles but it hugely decreased the performance of the accelerating-grid power supplies preventing the acceleration of further ions.

Thruster 'geometry' is the interaction of the physical design, magnetic and electrical fields that results in the successfully ionisation of a large number of atoms which are accelerated into a beam without significant ion impingement or loss of either neutral propellant atoms nor electrons. As you can imagine thruster geometry is extremely complex and requires (among other things) the solution of Poisson's equation. As I have demonstrated, however, good geometry is critical.

The lack of gas flow data prevents the calculation of thruster efficiency but needless to say it would be very low because of the poor electrical efficiency. Power losses were generated by ion impingement at the grids but the greatest power drain was from the highly inefficient filament electron source that dissipated most of its energy as heat.

In a future investigation the issue of chamber geometry would have to be addressed and would involve the investigation of different magnetic field shapes and strengths. To improve electrical efficiency and reduce thermal heating a new type of electron source would be required such as a hollow cathode. A new fabrication technique would need to be found to produce highly regular and symmetric accelerating grids to allow a multiple grid arrangement to be tested more thoroughly and finally an accurate method of gas flow control and measurement would be essential to allow a proper analysis of performance to be undertaken.

References

-
- ¹ Turner, M., "Rocket and Spacecraft Propulsion," Springer-Praxis 2000
 - ² Robert Goddard (1882-1945) Clark University, Massachusetts USA.
 - ³ Neuman D., "Magnetohydrodynamic Ion Drive as a main propulsion unit for a space vehicle," <http://www.physics.sfsu.edu/~dneuman/plasma.html>
 - ⁴ Child C. D., Phys. Rev., **32**, 498, 1911
 - ⁵ Brewer G. R., "Ion Propulsion: Technology and Applications," Gordon and Breach 1970
 - ⁶ Wirz R. et al, "Development and Testing of a 3cm Electron Bombardment Micro-Ion Thruster," IEPC Paper 01-343, 1998.
 - ⁷ Sr + H₂O ? Sr(OH)₂. "Research chemicals, metals and materials," Alfa Aesar 1999/2000
 - ⁸ <http://marr.bsee.swin.edu.au/~dtl/het408/projrad/projrad.html>
 - ⁹ <http://femm.berlios.de>

Bibliography

- Mark H. and Olson N. T., "Experiments in Modern Physics," McGraw-Hill 1966.
- Williams G. J. and Roman R. F., "High Specific Impulse, High Power Ion Engine Operation," AIAA Paper 2002-3838.
- Oh D. Y., "Aerospace America" article, Dec 2001.
- Patterson M. J. et al, "NEXT: NASA's Evolutionary Xenon Thruster," AIAA Paper 2002-3832. <http://fti.neep.wisc.edu/~jfs/neep533.lect31.99/plasmaProp.html>.
- Malik A. K., "Role of Magnetic Field in Kaufman Type Electrostatic Ion Thrusters," IEPC Paper 99-141.
- Jahn R. G. and Choueiri E. Y., "Electric Propulsion," Princeton University.